The Impact of Air Fences Geometry on Air Flow around an ICE3 High Speed Train on a Double Line Railway Track with Exposure to Crosswinds

M. Mohebbi and M. A. Rezvani[†]

School of Railway Eng., Iran University of Science and Technology, Tehran, 1684613114, Iran.

†*Corresponding Author Email: rezvani_ma@iust.ac.ir*

ABSTRACT

Reduction in weight adjoined with the increase in the railway vehicle speed of travel added to the deteriorating effects of the crosswinds on the running behavior of high speed trains. During the past decade, many researchers have concentrated on examining the aerodynamic force and moment coefficients for the trains. Varieties of studies regarding the effects of crosswinds on the trains are accomplished. However, the need to restrain strong winds from disturbing trains running safety is not completed. This research is concerned with finding a proper solution for attenuating the worrying effects of the winds that hit the trains. Installation of air fences on the sides of the railway tracks is investigated. To serve the purpose, a variety of air fences with different heights, with and without the edges on top of the fences, at a variety of the edge lengths and angles are studied. The study covers double routed railway track while the air fences are installed on either side of the track. The train can be on the leeward or windward line. The problem solving is based on the Lattice-Boltzmann method. This research pioneers in using this method for the said purpose. It is found that by inserting the fences and increasing their heights for up to 1m, the drag forces decrease to 40 percent and the rolling moment coefficients decrease to 15 percent. The presence of the edge can also decrease the drag force for about 55 to 120 percent and decrease the rolling moment coefficients for about 30 to 115 percent in some cases. Variations in percentages of reduction are due to the different angles and the lengths of the edges.

Keywords: High speed train; Air fence; ICE3; Double line railway track; Crosswind.

NOMENCLATURE

A	train cross section	H_w	fence height
BGK	Bhatnagar Gross Krook	H	train height
CFD	Computational Fluid Dynamic	ICE3	Intercity Express 3 Train
c_s	lattice sound speed	LBM	Lattice Boltzmann Method
c	lattice speed	LES	Large Eddy Simulation
c_x	side force coefficient	L	train length
c_y	lift force coefficient	L_E	edge length
c_{mz}	rolling moment coefficient	RANS	Reynolds Averaged Navier Stokes
c_{mr-lr}	lee-rail rolling moment coefficient	Re	Reynolds number
DES	Detached Eddy Simulation	SAS	Scale Adaptive Simulation
DNS	Direct Numerical Simulations	t	time
D_mQ_n	lattice form, m describes the dimension and n describes the model speed	URANS	Unsteady Reynolds Averaged Navier Stokes
$\vec{e}$	vector	$\vec{u}$	velocity vector
FDM	Finite Difference Method	W	train width
FEM	Finite Element Method	x,y,z	directions of coordination
FVM	Finite Volume Method	$\bar{x}$	space
$f_\alpha(\bar{x},t)$	particle distribution function at $\bar{x}$, t		
$f_\alpha^{eq}(\bar{x},t)$	equilibrium distribution function at $\bar{x}$, t	ω	collision frequency
		v	kinematic viscosity

ρ	density	ε	flow internal energy
δt	time step	α	edge angle

1. INTRODUCTION

There are reports about numerous studies that are concerned with the effects of crosswinds on the railway and road vehicles (Cheli *et al* 2011a, Cheli *et al* 2011b, Baker 2010). These studies also included experiments in order to estimate the transient aerodynamic loads on a normal railway vehicle that was subjected to crosswinds. The role of the angle of attack of the wind on the wagon and the position of the wagon on the bridge was estimated with details.

Suzuki and Hibino (2016) with constructing a full scale model of a train and viaduct at a windy area, attempted to measure the characteristics and aerodynamic forces acting on the train. They concluded that natural winds differ from the assumption of uniform flow.

In the recent era, researchers in the area of train aerodynamics are basically concerned on the aerodynamic drag force. The current trend in increasing the train speed of travel and reducing the train mass contributed to the destructive effects of the crosswinds on the trains. The plentiful of researches in the field of aerodynamics have generated fairly optimum designs for trains, road vehicles, airplanes and ships that also contain suitable maneuver powers. However, there is still lack of studies concerned with the issue of train safety against derailment under the effects of crosswinds. This was the case even when the first high speed train at a speed of 210 km/hr was introduced by Japanese (Zhou and Shen 2011). There was a negligence of the aerodynamic effects on the operational safety of trains, the distance between the railway tracks and the tunnel cross sections. Such effects were assumed of being very small (Suzuki *et al* 2003). Later on it was understood that this was a very important phenomena and it became an obstacle in increasing the train speed of travel in Japan, any further. By increasing the train speed of travel, the train resistance against movement increases and this in turn increases the train energy consumption. The train travel at high speed can generate pulses of high pressure air that distribute around and alongside the train. This can generate high pressure sound wave explosions that can even break the wagon glass windows. These strong pressure pulses have enough strength to overturn a double deck freight train. Research concerned with the train safety against derailment under the effect of crosswinds has not been very popular. Amongst the many reasons for such negligence one may notice some of the following (Chen *et al* 2009):

- With regard to aerodynamics, many researchers have been enthusiast of studying aeronautics, aerospace, hydrodynamic of ships and sea vessels. So far, there has not been enough interest for studying the train aerodynamics. The fact is that the trains' speed of travel is on the rise and it has been a long while since they started competing with airplanes. This generates the necessity for studying train aerodynamics in order to increase the running safety of the fleet and to add to the vehicle ride comfort.

- The interaction between the train-track-wind systems is complicated. It involves a variety of domains and subjects including railway engineering, vehicle design, aerodynamics, train derailment theories, bridge and tunnel engineering, soil and rock mechanics, etc. Therefore, train derailment under crosswind conditions is still a complex puzzle that lasted for too long throughout the passage of time (Chen *et al* 2005, Xiang and Zeng 2005).

- The high costs of operations, tests and computations and the complexity in duplicating the real scenarios under the real crosswind conditions and the train derailment are amongst the important issues that need to be included in this subject. Under such circumstances the use of the Computational Fluid Dynamic (CFD) methods for the prediction of the train aerodynamic performance in correspondence with the train running safety issues are very suitable (Guilmineau *et al* 2013, Krajnovic *et al* 2012, Mohebbi and Rezvani 2013).

Train overturning under crosswinds is dependent on two main parameters including the aerodynamic specifications of the track infrastructure and the rail vehicles. Regarding the infrastructure, locations with long bridges, viaducts and embankments are very important. Increasing the train speed of travel mixed with the reduction in the vehicle masses adds to the levels of anxiety, especially when the train travels on high grounds that are also susceptible to sudden winds. Therefore, it is important to collect proper and precise environmental information about the districts of interest.

Regarding the wagons, overturning due to the crosswinds specifically engages the first wagon in the train consist that is the most important and sensitive part in the train combination. This is due to the fact that the first wagon is exposed to the highest aerodynamic loads (Diedrichs 2008).

There are reports about the effects of crosswinds on trains in recent years. Amongst them are review reports by Baker *et al* (2009), Baker (2014a, 2014b) and Raghunathan *et al* (2002), Avadiar *et al* (2016) and He (2014), Premoli *et al* (2015). However, there seems to be a lack of research regarding the train resistance against crosswinds and reducing the deteriorating effects of winds on the moving trains. The focus of the studies was more about obtaining the aerodynamic forces and moments' coefficients. Amongst the solutions to reduce the speed of wind that hits the trains is the use of air fences.

A few studies have been concerned with the protective effects of fences for roads and railways. A wind tunnel test and a Large Eddy Simulation (LES) study were used to investigate the protective effect of porous windbreak on road vehicles against the wind (Chu *et al* 2013). They found that the porous windbreaks can significantly reduce the side force coefficient of the vehicles.

A wind tunnel study on the wind barrier effects on a train-bridge system is reported (Guo *et al.* 2015). They found that the side force and the rolling moment coefficients of the vehicle are efficiently reduced by a single side wind barrier.

It is the purpose of this research to investigate the effects of air fences on the coefficients of the aerodynamic forces and moments on the train surfaces. This study considers a double route railway track with air fences on either side of the track and a high speed train that travels along the track at certain speed. The effect of the train on the windward and leeward track is examined. This work includes computations involving a variety of air fences with different heights and edges at different angles. The first step involves computations for a three dimensional model of an interstate high speed train ICE3 on a flat ground. This result will be used for the validation of the model by comparing the results with the ones that are available in the standard document EN14067-6:2010 and in the report by Schober *et al* (2010). The computations will then involve a two dimensional model in order to reduce the processing time. The two dimensional model will be validated by comparing with the three dimensional model. The two dimensional model will be used for further processing involving the air fences and their effects on the train aerodynamic coefficients.

2. THEORETICAL PERCEPTIONS

In computational analyses of fluid flow problems, methods based on discretizing the Navier-Stocks equations such as the Finite Volume Method (FVM), Finite Element Method (FEM), Finite Differences Method (FDM), etc. are widely used for research and computations (Feng *et al* 2006, Benim *et al* 2006). Almost all fluid flows in engineering applications are turbulent and contain a wide spectrum of different scales of vortices of particles. The solution to these types of issues by using the methods such as Direct Numerical Simulation (DNS) for the domains of Reynolds' number is not practical since it needs very strong computation resources while most computers do not accommodate such capabilities. Therefore, methods such as Large Eddy Simulation (LES) and Reynolds averaged Navier-Stocks (RANS) can be used.

LES can only solve large structures to save most turbulent energy that is found in large vortices while smaller structures are modeled by using sub-grid scale models (Sagaut 2004). Nevertheless, LES models still need resolutions and proper computation resources that stop the usual industrial application of these methods.

Fragner and Deiterding (2016) investigated the crosswind stability for a simplified train model at a scale of 1:25 by parallel LES with incompressible solvers from the Openfoam package. They found that the Lattice Boltzmann Method (LBM) provides more accurate time averaged force predictions, while the computation time is reduced.

Recent developments such as DES (Detached Eddy Simulation), SAS (the Scale-Adaptive Simulation) or one of the many combined models such as Unsteady Reynolds Averaged Navier Stokes (URANS) or Large Eddy Simulation (LES) model show that the need exists for practical advanced methods that produce the best solutions directly or together with a turbulence model over a lattice space (Spalart 2000, Menter *et al* 2003).

Other organized methods in airfoil theory, such as the panel method and the lift surface method, with practical results can happen only under special circumstances. These are attractive research subjects that are always under review and improvements about them are expected.

In comparison with the classical computational fluid dynamic methods that are based on the Navier-Stocks equations, there is also a method that is based on the Boltzmann Gas Kinematic equations that describes the molecular motions. This is called the Lattice-Boltzmann method (McNamara and Zanetti 1998). Although, this method is not yet as popular as the other methods, but for the last three decades application of LBM as a proposed computational trend for solving the fluid dynamic problems has had rapid gross (Succi 2001, Sukop and Thorne 2006, McNamara and Zanetti 1998). A domain with fair popularity for this method is the prediction of small scale single phase and multi-phase flow, flow with low and high Reynolds' numbers, complex geometries, etc. (Xu *et al* 2009a, Suga *et al* 2009). Here, turbulence is considered as an important issue.

Amongst other applications of LBM is the solution to problems with complex flows that need a very good Lattice resolution for problems of very large sizes (Xu *et al* 2009b). Regarding LBM Xu *et al* used two equations turbulence method LES (Large Eddy Simulation). LES formulation is based on the sub grid-scale viscosity that gets wider applications (Sagaut 2004). This is used as a normal proposal in LBM (Guan and Wu 2009). The common interest is in the applications with high Reynolds' numbers. The most common formulation for Lattice Boltzmann method is based on BGK (Bhatnagar-Gross-Krook) estimation (Bhatnagar *et al* 1954).

For the purposes of the present research a version of this model that is suitable for compressible flows that was suggested by Zou *et al* (1995) is used.

2.1 Discretized Equations

In Lattice-Boltzmann method, rearrangement of the particles happens during the collision and the flowing stages and the new distribution functions are then calculated. The general configurations of

these lattices are in the form of D_mQ_n that m describes the dimension and n describes the model speed. Some examples for one, two and three dimensional cases include D_1Q_3, D_1Q_5, D_2Q_9, D_3Q_{15}, D_3Q_{19}. The present research uses a two dimensional nine speed lattice model D_2Q_9 that is the most popular lattices amongst the two dimensional equations. The configuration of D_2Q_9 lattice and the corresponding speeds are presented in Fig. 1.
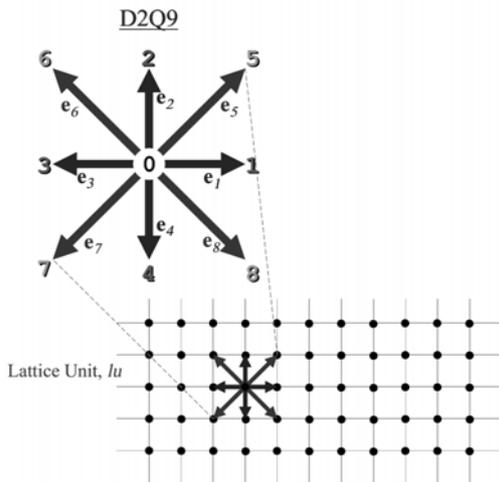
Fig. 1. Lattice D_2Q_9 and the corresponding speeds (Sukop and Thorne 2006).

The evolved discretized lattice-Boltzmann equations that are normally solved in the two consecutive steps of collision and streaming are as in Eq. (1):

The collision step:

$$\tilde{f}(\bar{x},t+\delta t) = f(\bar{x},t) - \omega[f(\bar{x},t) - f^-(\bar{x},t)] \tag{1}$$

where $f^-(\bar{x},t)$ is the equilibrium distribution function.

The streaming step:

$$f(\bar{x} + \bar{e}\,\delta t, t + \delta t) = \tilde{f}(\bar{x}, t + \delta t) \tag{2}$$

Before determining the equilibrium distribution function the corresponding variables must be defined. Calculation of such variables is an important step for discretizing the Boltzmann equation.

The collision frequency ω is defined as;

$$\omega = 1 / \left(v / (c\,\delta t) + 1/2 \right) \tag{3}$$

where c_s is the lattice sound speed that is defined as in Eq. (4);

$$c_- = c / \sqrt{3} \tag{4}$$

where c is the lattice speed;

$$c = \delta / \delta t \tag{5}$$

The collision frequency specifies the fraction of particles that collide in a small amount of volume during a time interval δt according to the collision interval theory (Huang 1987).

The nine discrete model speeds are defined as in Eq. (6);

$$\vec{e}_\alpha = c \begin{bmatrix} 0 & 1 & 0 & -1 & 0 & 1 & -1 & -1 & 1 \\ 0 & 0 & 1 & 0 & -1 & 1 & 1 & -1 & -1 \end{bmatrix} \tag{6}$$

The equilibrium distribution function is according to Eq. (7);

$$f^- = w \left[\rho + \frac{3}{c}\vec{e}\cdot\vec{u} + \frac{9}{2c}(\vec{e}\cdot\vec{u}) - \frac{3}{2c}\vec{u}\cdot\vec{u} \right] \tag{7}$$

with;

$$w_\alpha = \begin{cases} 4/9 & for \;\; \alpha = 0 \\ 1/9 & for \;\; \alpha = 1,2,3,4 \\ 1/36 & for \;\; \alpha = 5,6,7,8 \end{cases} \tag{8}$$

The macroscopic limits are obtained through the following equations:

$$\rho = \sum f = \sum f^- \tag{9}$$

$$\rho\vec{u} = \sum_{i=0}^{8}\vec{e}_\alpha f_\alpha = \sum_{i=0}^{8}\vec{e}_\alpha f_\alpha^{eq} \tag{10}$$

$$\rho\varepsilon = \frac{1}{2}\sum_{i=0}^{8}(\vec{e}_\alpha)^2 f_\alpha = \frac{1}{2}\sum_{i=0}^{8}(\vec{e}_\alpha)^2 f_\alpha^{eq} \tag{11}$$

$$\bar{p} = \rho c_s^2 \tag{12}$$

The size of the time step δt is obtained by using the same method for obtaining the lattice speed c and the lattice sound speed c_s as in Eqs. (4) & (5).

The turbulence model is considered based on the very large eddy simulation (VLES) that simulates the resolvable flow scales by using an RNG form of k-ε equations with proprietary extensions to attain VLES time accurate physics (Chen *et al* 1987).

This is being noted that the Lattice Boltzmann Method tenants a perceptual vision of an advantageous delegation of fluid turbulence over the solution of the Navier Stokes equations due to its computationally efficient formalization (Chen *et al* 2003).

3. MODELING

3.1 Geometrical Model

When studying aerodynamic of trains, their real geometries are considered as too complicated. Therefore, there is a preference for replacing them with simplified models. The model of interest to this research is a copy from ICE3 German high speed train with simplifications that are

recommended by EN14067-6:2010 under the title of railway-Aerodynamic applications Section 6: Requirements and test methods for crosswind evaluations.

The German ICE3, or Intercity-Express 3, is the third generation of the ICE, with some radical changes to previous generations and a member of electric multiple unit (EMU) high speed trains operated by Deutsche Bahn.

The ICE 3 high speed train is an eight car train where the cars are self-propelled. The carriages are shorter and narrower compared with the ICE 1 and ICE 2 types. The front shape is more streamlined, and instead of the two rectangular front windows, it encompasses one large oval window. The passengers in the first and the last car have the commodity to look out through the cab. The tilting InterCity train ICT for classic lines has the same general front arrangement, but with a steeper, less streamlined shape.

Aerodynamic coating of the pantographs similar to Japanese Shinkansen trains is installed on all ICE 3 carriages to reduce the wind noise and air resistance.

The provided model of ICE3 train for testing based on EN14067-6:2010 standard includes a front wagon plus the next half wagon with an inter-car-gap. This is due to the fact that the structure of the downstream flow at a certain distance from the train nose is fairly constant and the reduction in length is not much effective for the flow (Khier *et al* 2000). The model is on a 1/7 scale and is according to the standard. The reference moment point is on the ground surface along the length of the train. The aerodynamic forces and moments coefficients are calculated based on the constant reference surface. This surface is proportional to the train cross section of $A=10m^2$ and the reference length of $L=3m$. This defines the width of the model train that is compatible with the TSI normalization (OJEU 2008).

3.2 Computational Domain

As the first step, the calculations are performed in a three dimensional space and the aerodynamic forces and moments coefficients for the model train are calculated. The computational domain for such a purpose is presented in Fig. 2.
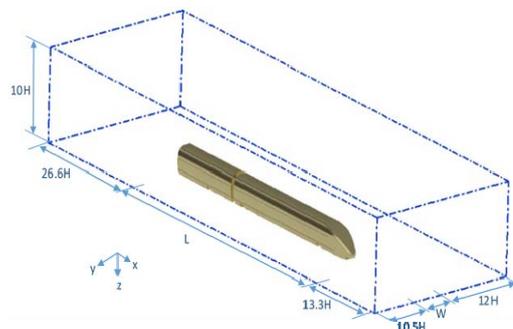
Fig. 2. Three dimensional computational model (The dimensions are adjusted to the length, width and height of the train).

The domain is in the shape of a rectangular cuboid with the sizes that are also parametrically presented in this figure. The distance to the boundaries are taken large enough in order to make sure that the speed and pressure domains at the entrance are uniform. This will also allow the flow to develop during the time that it needs to reach to the train. The model is also at the proper distance from the roof and the sides of the domain in order to minimize the so called "near wall effects". The distance between the train and the ground surface is 0.065 times the train height that is according to the 235mm gap that is recommended in EN14067-6:2010 standard.

After solving for the model in three dimensions, the results are validated by comparing with the results in EN14067-6:2010 standard and the results that are reported by Schober *et al* (2010). Then the next step for the two dimensional analysis starts. The domain that is used for the two dimensional computations is presented in Fig. 3. This figure also illustrates the air fences.

In Fig. 3, H, W, H_F, L_F, α represent the train height, the train width, the air fence height, the length of the air fence edge, and the air fence edge angle, respectively. Also the coordinate system is according to the EN14067-6:2010 recommendations. It needs to be reminded that the dotted train replaces the model train when studying the effect of the model train on the computational domain when it is installed on the leeward route.

3.3 Boundary Conditions

There are many possibilities for combining the train and the crosswind velocities. But for the high speed train applications, the wind perpendicular to the train simulates the worst wind conditions. This comes from the recommendations that the changes in the characteristic wind curve (CWC) are relatively small for high speed trains (Baker 1991).

Therefore, in order to consider the more realistic scenarios for the high speed trains the worst case setting is considered. This translates into the airflow for crosswinds at 90 degree of yaw relative to the train direction of travel. The flow of air enters at a uniform speed of 80 m/s. The boundary conditions are considered as no-slip at the train surface and the ground surface. This is equivalent to zero velocity. The Reynolds' number based on the effective speed of the crosswind and the train height is $Re=1.6\times10^7$. The symmetrical boundary conditions on the upper and the side walls are considered. At the exit, the homogeneous Neumann boundary condition is assumed that is equivalent to the zero pressure gradients. This allows the flow to exit without influencing the upstream flow. As far as this type of modeling is concerned, taking certain recommended distances at the front and the back of each obstacle is a well-liked and accepted phenomena. On the ground and the solid surfaces, the non-equilibrium wall fences are used in order to estimate the quantity of disturbance.
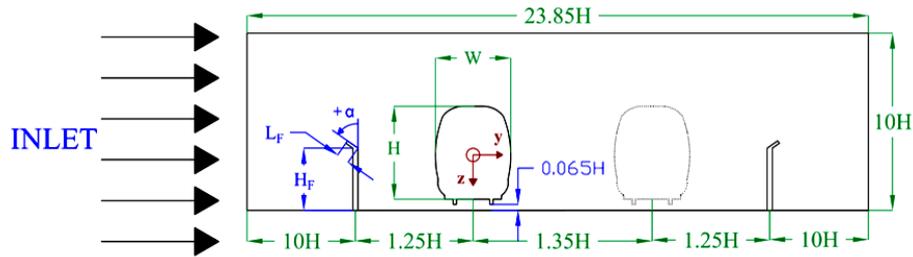
Fig. 3. Cross section of a train on a double route railway track with air fences.

The LBM is a mesoscopic scale method that is not using the meshing procedure that is available in the classical CFD methods such as FVM and FEM. The major significant difference between LBM and the other classical methods is that the LBM is a straightforward method in complicated geometries. Therefore, LBM replaces the mesh generation in the other methods with domain discretization within a lattice structure

4.   RESULTS AND DISCUSSIONS

The first step of the computations is for a three dimensional case. The results of the air flow over ICE3 under crosswind at deviation angles of 0º, 30º, 60º, 90º are presented in Figs. 4&5.

For validation purposes, these results are compared with the results that are reported in EN14067-6:2010 standard and the results that are reported by Schober *et al* (2010). The standard test and Schober *et al* (2010), performed the study of the flow over an ICE3 under different wind tunnel test setup with similar adjustments.

It is clear that the results are very compatible. There are only some small differences for the aerodynamic coefficients at the deviation angle of 60º. This can be due to the end car effect and the inter car gap that is modeled in the CFD analysis. According to Schober *et al* (2010), reaching at the coefficients that are reported in the standard are very difficult. Eventually, it can be suggested that the results of the modeling by using the Lattice-Boltzmann method are comparable with the results from the standard and the results that are reported by Schober *et al* (2010). Therefore, the modelling is valid.

After this stage, the modeling is continued in two dimensions and the aerodynamic coefficients are recalculated. The results from the two dimensional modeling are compared with the three dimensional molding and the EN14067-6:2010 standard results. The data are provided in Fig. 6.

Also, in order to present a better comparison between the calculated results, an error percentage comparison relative to the standard EN14067-6:2010 is provided in Table 1.

From the results, it is obvious that the differences between the forces and the moments' coefficients are at a minimum. This validates the procedure for moving to the next stages in the computations.

Table 1 An error percentage comparison of the aerodynamic coefficients for the high speed train ICE3 under crosswind (at a deviation angle of 90º)

	2D CFD (LBM)	3D CFD (LBM)
c_x	22 %	24 %
c_y	-13 %	-3 %
c_{mz}	-6 %	4 %
$c_{mr\text{-}lr}$	-5 %	6 %

The third stage involves studying the effects of air fences that are installed near the train tracks. As already stated, the aim of this research is to investigate the effects of air fences on the flow of air that hits the high speed trains. To serve the purpose, the modelling includes air fences on either side of the double routed railway track. The effects of crosswinds on the train surfaces when the train is on the leeward or on the windward sides are considered. The study includes air fences with a height of one to three meters. Also the effects of edges at the top of the air fence at the angles of ±45º (from the vertical axis) and a variety of edge lengths in the range of 0.5-1m are considered. The results are presented in Fig. 7.

With the increase in the air fence height up to 1m, the aerodynamic force coefficient decreases and afterward it exhibits an increasing trend up to the air fence height of 2m. This coefficient then decreases with further increase in the air fence height. The results for both cases of the train in the leeward and the windward sides are the same.

The effect of the air fence edge on the reduction of this coefficient is considerably higher. This is rather clear from the results and as the length of the air fence edge increases the reduction in this coefficient increases. Regarding the edge angle on top of the air fence, an angle of +45º is more effective in reducing the drag coefficient compared with the edge angle of -45º.

The lifting force coefficient increases with the increase of the air fence height. The rate of this increase is very fast up to the air fence height of 2m and it becomes fairly constant afterward. The addition of the edges on the air fence reduces the

(a)

(b)

(c)

(d)

(e)

(f)
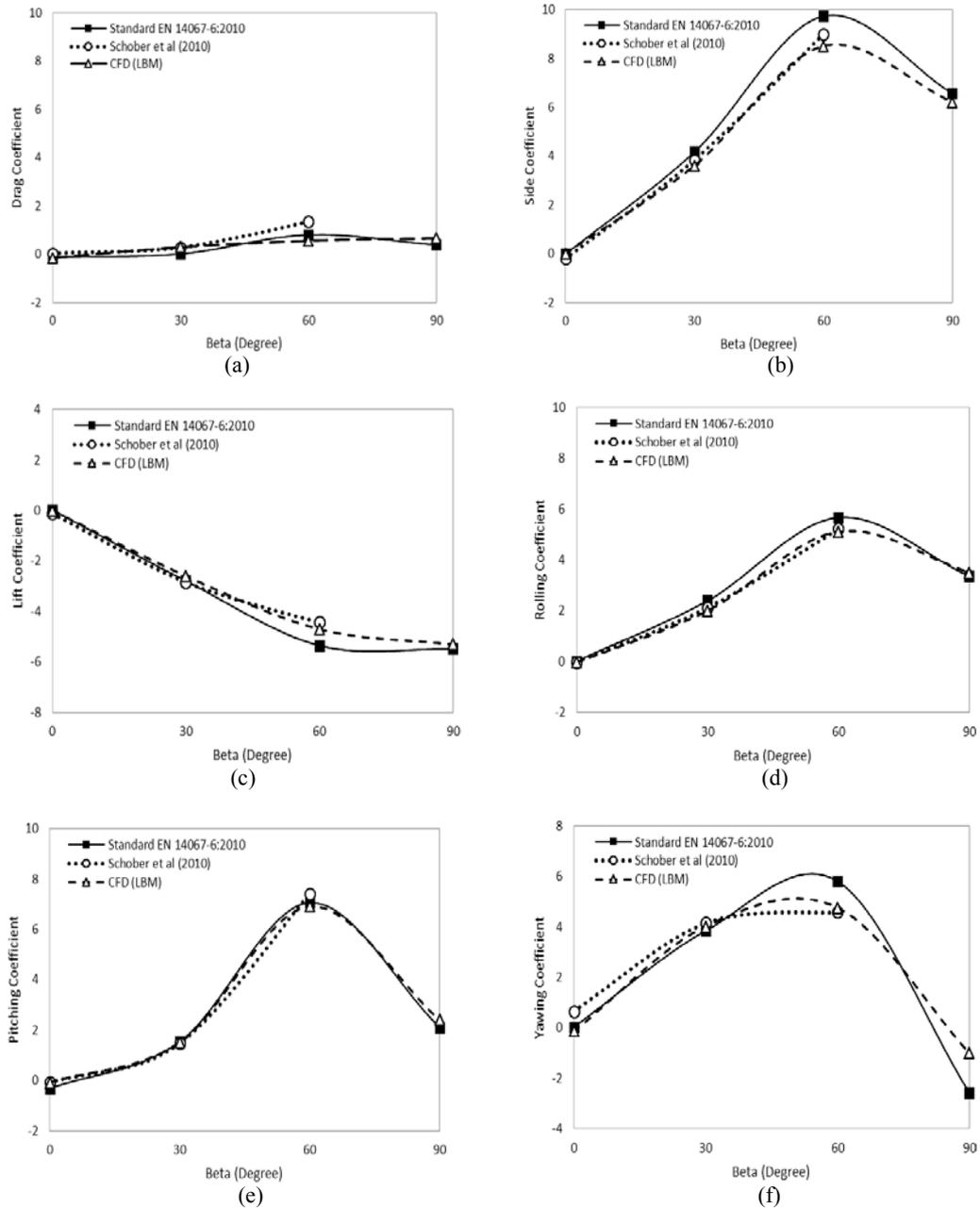
Fig. 4. Aerodynamic force and moment coefficients at deviation angles of 0º, 30º, 60º, 90º for a 3D model of a high speed train ICE3. (a) Drag Coefficient, (b) Side Coefficient, (c) Lift Coefficient, (d) Rolling Coefficient, (e) Pitching Coefficient, and (f) Yawing Coefficient.
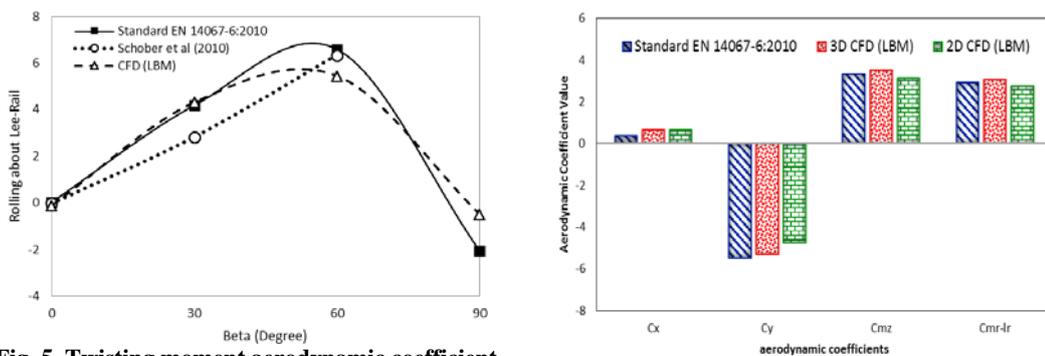
Fig. 5. Twisting moment aerodynamic coefficient around leeward rail at deviation angles of 0º, 30º, 60º, 90º for a three dimensional model of a high speed train ICE3.

Fig. 6. A comparison for the aerodynamic coefficients for the high speed train ICE3 under crosswind (at a deviation angle of 90º).

(a)

(b)

(c)

(d)

(e)

(f)

(g)

(h)
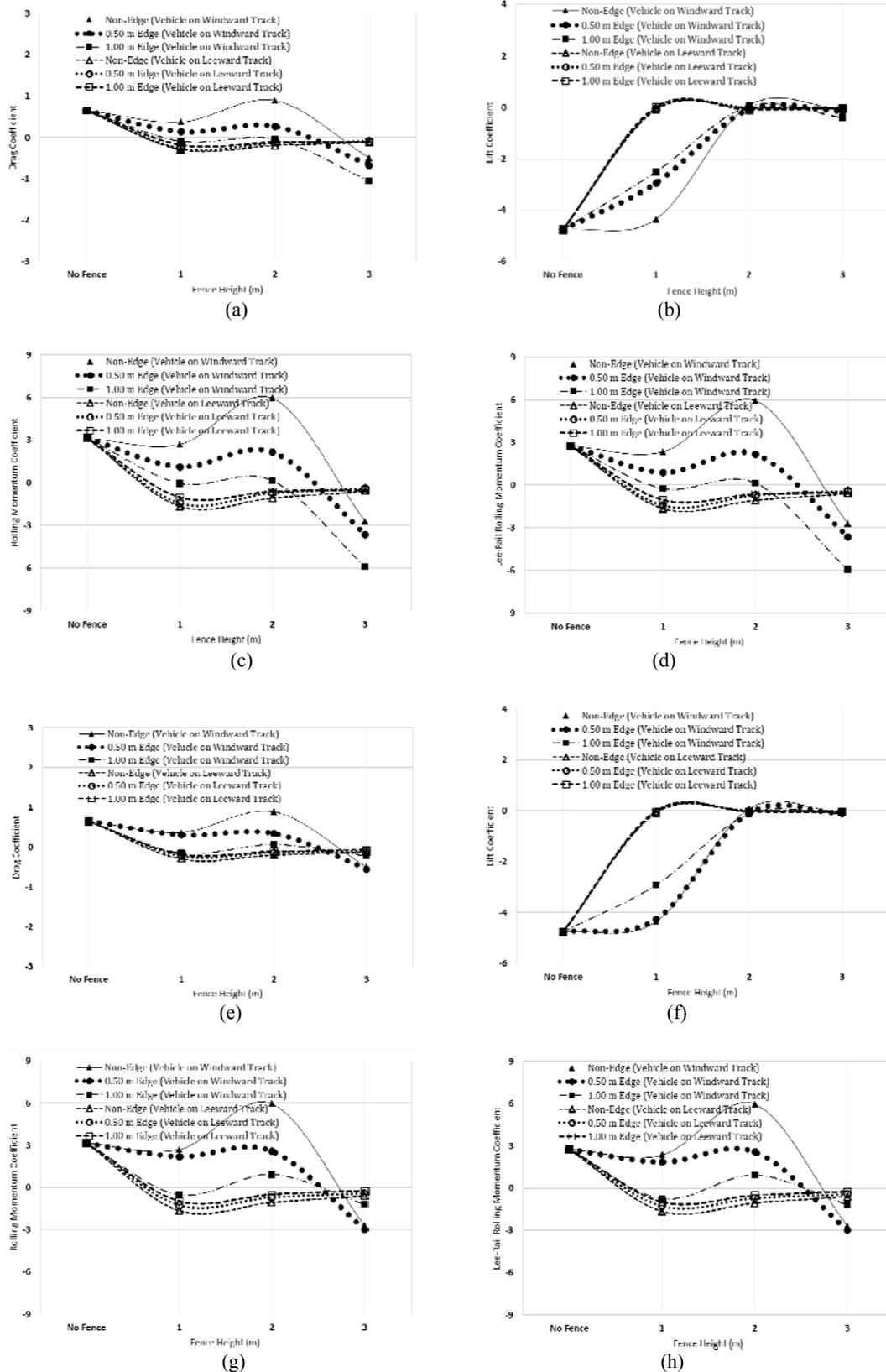
Fig. 7. Aerodynamic coefficients for the model train at crosswinds at the presence of the air fences of different heights, length and edge angles. (a) Drag Coefficients for Edge at +45º, (b) Lift Coefficients for Edge at +45º, (c) Rolling Moment Coefficients for Edge at +45º, (d) Lee-Rail Rolling Moment Coefficients for Edge at +45º, (e) Drag Coefficients for Edge at -45º, (f) Lift Coefficients for Edge at -45º, (g) Rolling Moment Coefficients for Edge at -45º, (h) Lee-Rail Rolling Moment Coefficients for Edge at -45º.

rate of the increase of the force coefficient. However, the edge angle is not very influential. Also, when the train is on the leeward line the rate of the increase turns to be higher.

The rolling moment coefficient is like the drag force coefficient (a reminder that in the two dimensional model the drag coefficient is like the side coefficient in the three dimensional model). The side force is basically a result of the pressure differences between the two sides of the train. The side force increases the rail/wheel load on the leeward side and also increases the contact force between the wheel/rail. The higher amounts of this force cause the wear of the wheels and rail and also can cause derailments and overturning of the vehicle in some instances. As it is clear from the results, the trend in the rolling moment coefficient is like the lift force coefficient. This coefficient has a decreasing trend up to the height of 1m. Afterward and up to the height of 2m it increases and beyond 2m it again endures a reduction trend. The sizes of this coefficient compared to the drag force coefficients are higher. The rolling moment can be considered as a result of both lift and drag forces while the effect of the drag force is considerably higher. Regarding the effect of the edge angle on the rolling moment coefficient it is found that the edges with the positive angle are more effective in reducing these coefficients compared with the edges with negative angles.

The lee-rail rolling moment is responsible for removing the wheel/rail load on the leeward side. This is the coefficient with the most novel effect on the stability of the trains against the crosswinds. This coefficient acts similar to the rolling moment coefficient and follows the same behavior. The presence of the edge on top of the air fence slows down the variations of this coefficient. With the increase in the length of the edge, this coefficient reduces. The behavior of the train on the leeward route is different from the train on the windward route, when the height of the air fence is over 2m. Such difference can be attributed to the presence of the different flow separation phenomena on the trains in the two different positions. The influence of the positive and the negative edge angles is the same as for the rolling moment coefficients.

The pattern of the flow in the domain of interest is constructed by using the vorticity contours and the results are presented in Fig. 8.

As expected, while the train is on the windward route the large flow separation zones are observed on the windward side of the train and for the train on the leeward route, such flow separation is weaker. The recirculation zone due to the Eddy currents near the train body increases and then slowly moves away from the surface and develops in the wake leeward zone. The flow separation happens on both the upper and the lower leeward edges. This causes a low pressure zone on the leeward side of the train that is due to the presence of the sever side forces and rolling moments.

(a)

(b)

(c)

(d)

(e)

(f)

(g)

(h)
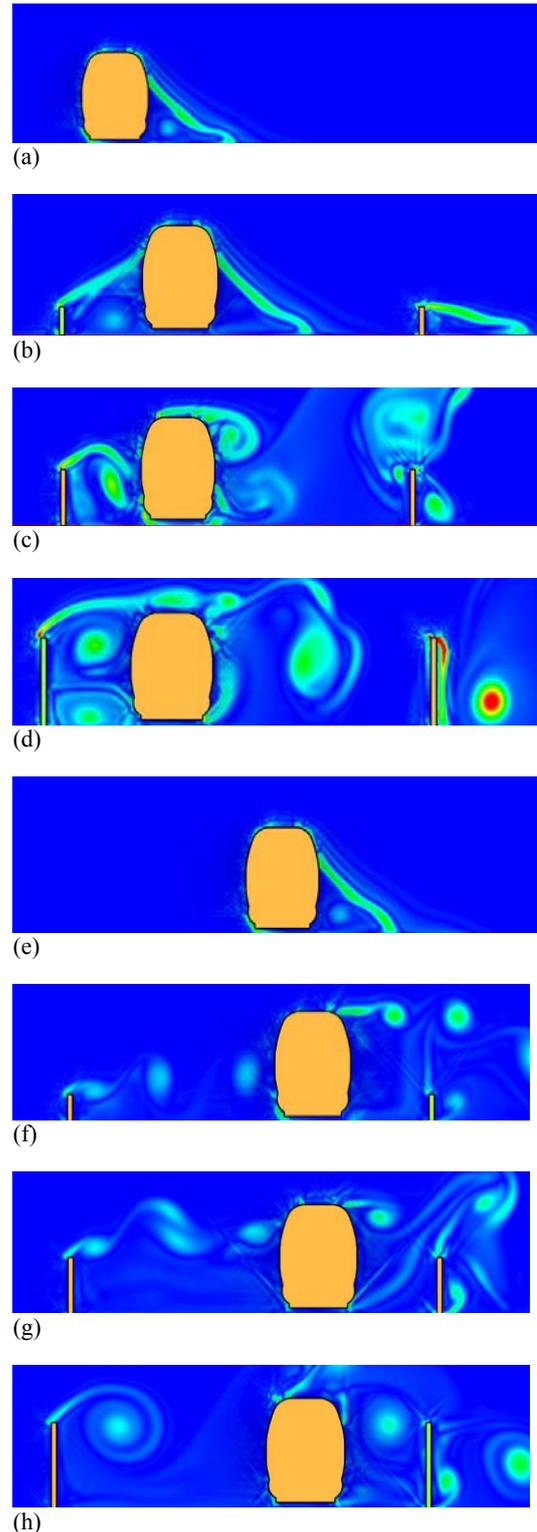
Fig. 8. Vorticity contours for the two dimensional models including air fences with different heights. (a) No Air fence installed and vehicle on windward track, (b) H_w = 1.0m and vehicle on windward track, (c) H_w = 2.0m and vehicle on windward track, (d) H_w = 3.0m and vehicle on windward track, (e) No Air fence installed and vehicle on leeward track, (f) H_w = 1.0m and vehicle on leeward track, (g) H_w = 2.0m and vehicle on leeward track, (h) H_w = 3.0m and vehicle on leeward track.

(a)

(b)

(c)

(d)

(e)

(f)

(g)

(h)
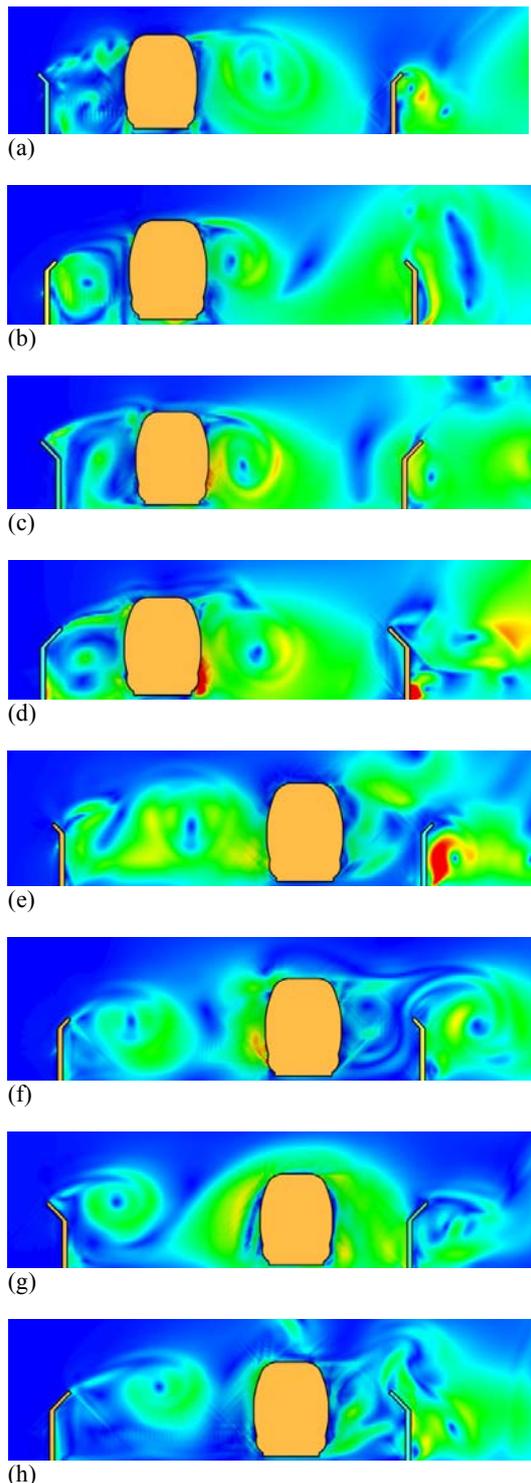
Fig. 9. Turbulence intensity contour for the two dimensional modelling including the air fences with a height of H_w = 2.0m. (a) α = +45°, L_E = 0.5m and vehicle on windward track, (b) α = -45°, L_E = 0.5m and vehicle on windward track, (c) α = +45°, L_E = 1.0m and vehicle on windward track, (d) α = -45°, L_E = 1.0m and vehicle on windward track, (e) α = +45°, L_E = 0.5m and vehicle on leeward track, (f) α = -45°, L_E = 0.5m and vehicle on leeward track, (g) α = +45°, L_E = 1.0m and vehicle on leeward track, (h) α = -45°, L_E = 1.0m and vehicle on leeward track.

The turbulence intensity that is often referred to as the turbulence level is the root mean square of the turbulent velocity fluctuations to the man velocity. Figure 9 presents an example for a few air fences with a height of 2 meter. From this set of results it is observed that air fences with the edge angle of +45° are more effective in reducing the intensity of turbulence and the speed of wind that hits the train compared with the edge angle of -45°. Also, the longer edges are more effective compared with the shorter ones. This is valid for both cases of the ICE3 train on the leeward and the windward routes. Also, the turbulence intensity at the vehicles on the leeward track is very weaker than the vehicles on the windward track. This is also a confirmation of the results that are already discussed in the prior sections of this article.

5. CONCLUIONS

The effects of installing air fences, on either side of a double route railway track, on the aerodynamic performance of a high speed intercity train (ICE3) are investigated. A variety of air fences with the heights ranging from 1m to 3m, with and without edges on the top of the fence, with the edge lengths of 0.5m and 1.0m, and the edge angles of -45° and +45° are examined. The Computational Fluid Dynamic (CFD) based on the Lattice-Boltzmann method of solution is used. Using such a method, very accurate results are generated. The major outcome of this research is listed as follows;

- When increasing air fences' heights for up to 1m, the drag force decreases to about 40 percent and the rolling moment coefficient decreases to about 15 percent. By further increasing the air fences heights for up to 2m these coefficients increase. They start decreasing for any further increase in the height.

- The presence of the edge causes decrease in the drag forces to somewhere between 55 to 120 percent and decrease in the rolling moment coefficients to about 30 to 115 percent in some cases. The variations in such coefficients are due to the different angles and lengths of the edges. The increase in the edge length increases the rate of such decrease.

- The edge angle of +45° on top of the air fence is more effective in reducing the aerodynamic drag forces and the rolling moment coefficients compared with the edge angle of -45°. The positive edge angles can be up to 30% more effective.

- Considering the lift force coefficient, the rate of increase when the train is on the windward side is lower compared with the case when the train is on the leeward side.

- While studying the disturbance contour plots for air fences with different geometries, it became clear that the edge angle of +45° is more effective in reducing the rate of disturbance and the speed of wind that hits the train. Such condition exists for the case of an ICE3 on the

leeward as well as on the windward side of the track.

ACKNOWLEDGEMENTS

REFERENCES

Avadiar, T., J. Bell, D. Burton, H. Cormaty and C. Li (2016). Analysis of high-speed train flow structures under crosswind *Journal of Mechanical Science and Technology* 30, 3985-3991.

Baker, C. (2014). A review of train aerodynamics Part 1 – Fundamentals *The Aeronautical Journal* 118.

Baker, C. (2014). A review of train aerodynamics Part 2 – Applications *The Aeronautical Journal* 118.

Baker, C. J. (1991). Ground Vehicles in High Cross Winds, Part 1: Steady Aerodynamic Forces *Journal Fluids Structure* 5: 69-90.

Baker, C. J. (2010). The simulation of unsteady aerodynamic cross wind forces on trains *Journal of Wind Engineering & Industrial Aerodynamics* 98(2):88–99.

Baker, C., F. Cheli, A. Orellano, N. Paradot, C. Proppe and D. Rocchi (2009). Cross wind effects on road and rail vehicles *Vehicle System Dynamics* 47, 983-1022.

Benim, A. C., A. Nahavandi, P. J. Stopford and K. J. Syed (2006). DES LES and URANS Investigaton of Turbulent Swirling Flows in Gas Turbine Combustors *WSEAS Transactions on Fluid Mechanics* 1:465-472.

Bhatnagar, P., E. Gross and M. Krook (1954). A model for collisional processes in gases I: small amplitude processes in charged and neutral one-component system *Physics Review* 94, 511-525.

Cheli, F., R. Corradi, E. Sabbioni and G. Tomasini (2011a). Wind tunnel tests on heavy road vehicles: Cross wind induced loads—Part 1 *Journal of Wind Engineering & Industrial Aerodynamics* 99(10), 1000–1010.

Cheli, F., F. Ripamonti, E. Sabbioni and G. Tomasini (2011b). Wind tunnel tests on heavy road vehicles: Cross wind induced loads— Part 2 *Journal of Wind Engineering & Industrial Aerodynamics* 99(10), 1011–1024.

Chen H, Kandasamy S, Orszag S, Shock R, Succi S and Yakhot V (2003) Extended Boltzmann kinetic equation for turbulent flows *Science* 301:633–6.

Chen, R. L., Q. Y. Zeng and D. J. Li (2005). Dynamic Analysis of Train-Track-Bridge Wind System *New York: Science Press* 40-44.

Chen, R. L., Q. Y. Zeng, X. G. Zhong, J. Xiang, X. G. Gang and G. Zhao (2009). Numerical study on the restriction speed of train passing curved rail in cross wind *Sci China Ser E-Tech Sci* 52, 2037-2047.

Chen, Y. S. and S. W. Kim (1987). Computation of turbulent flows using an extended k-turbulence closure model. *NACA CR-179204.*

Chu, CH. E., CH. Y. Chang, CH. J. Huang, T. R. Wu, CH. Y. Wang and M. Y. Liu (2013). Windbreak protection for road vehicles against crosswind *Journal of Wind Engineering and Industrial Aerodynamics* 116, 61-69.

Diedrichs, B. (2008). Aerodynamic calculations of cross wind stability of a high-speed train using control volumes of arbitrary polyhedral shape *Milan: the VI international colloquium on: bluff bodies aerodynamics & applications (BBAA).*

Feng, J., F. K. Benra and H. J.Dohmen (2006). Numerical Investigation of Radial Gap Influence on Diffuser Induced Impeller Flow *WSEAS Transactions on Fluid Mechanics* 1, 473-479.

Fragner, M. M. and R. Deiterding (2016). Investigating cross-wind stability of high-speed trains with large-scale parallel CFD *International Journal of Computational Fluid Dynamics.*

Guan, H. and Wu C. J. (2009). Large eddy simulations of turbulent flows with lattice Boltzmann dynamics and dynamical system sub-grid models *Science in China Series E* 52, 670-679.

Guilmineau, E., O. Chikhaoui, G. Deng and M. Visonneau (2013). Cross wind effects on a simplified car model by a DES approach *Computational Fluids* 78, 29-40.

Guo, W. W., Y. J. Wang, H. Xia and SH. Lu (2015) Wind tunnel test on aerodynamic effect of wind barriers on train-bridge system *Science China Technological Sciences* 58, 219-225.

He, X. H., Y. F. Zou, H. F. Wang, Y. Han and K. Shi (2014). Aerodynamic characteristics of a trailing rail vehicles on viaduct based on still wind tunnel experiments *Journal of Wind Engineering and Industrial Aerodynamics* 135, 22-33.

Huang, K. (1987). Statistical Mechanics *John Wiley & Sons Inc. New York.*

Khier, W., M. Breuer and F. Durst (2000). Flow structure around trains under side wind conditions: A numerical study *Journal of Computers and Fluids* 29, 179-195.

Krajnovic, S., P. Ringqvist, K. Nakade and B.

Basara (2012). Large eddy simulation of the flow around a simplified train moving through a crosswind flow *Journal of Wind Engineering & Industrial Aerodynamics* 110, 86-99.

McNamara, G. and G. Zanetti (1988). Use of the Boltzmann Equation to Simulate Lattice Gas Automata *Physics Review Letter* 61, 2332–2335.

Menter, F. R., M. Kuntz and R. Bender (2003). A scale-adaptive simulation model for turbulent flow predictions *AIAA Paper* 2003-0767.

Mohebbi, M. and M. A. Rezvani (2013). Numerical Calculations of Aerodynamic Performance an Regional Passenger Train at Crosswind Conditions *Journal of Vehicle Structures & Systems* 5, 68-74.

OJEU (Official Journal of the European Union) (2008). Technical specification for interoperability of high speed rolling stock TSI/HS-RST-L64-7/3/2008:2008.

Premoli, A., D. Rocchi, P. Schito, C. Somaschini and G. Tomasini (2015). A Computational Fluid Dynamics Study on the Relative Motion Effects for High Speed Train Crosswind Assessment *Proceedings of the Fifteenth International Conference on Civil, Structural and Environmental Engineering Computing,* Civil-Comp Press, Stirlingshire, Scotland.

Raghunathan, R., H. D. Kim, T. Setoguchi (2002). Aerodynamics of high-speed railway train *Progress in Aerospace Sciences* 38:469-514

Sagaut, P. (2004). Large Eddy simulation for incompressible flows (2ⁿᵈ Ed) *Berlin: Springer-Verlag.*

Schober, M., M. Weise, A. Orellano, P. Deeg and W. Wetzel (2010). Wind tunnel investigation of an ICE 3 endcar on three standard ground scenarios *Journal of Wind Engineering & Industrial Aerodynamic*.

Spalart, P. R. (2000). Strategies for turbulence modelling and simulations *International Journal of Heat and Fluid Flow* 21, 252-263.

Succi, S. (2001). The Lattice Boltzmann Equation for Fluid Dynamics and Beyond *Oxford: Clarendon Press.*

Suga, K., T. Tanaka, Y. Nishio and M. Murata (2009). A boundary reconstruction scheme for lattice Boltzmann flow simulation in porous media *Progress in Computational Fluid Dynamics* 9, 201-207.

Sukop, M. C. and D. T. Thorne (2006). The Lattice Boltzmann Modelling *Springer.*

Suzuki, M. and Y. Hibino (2016). Field tests and wind tunnel tests on aerodynamic characteristics of train/vehicles under crosswinds *QR of RTRI* 57, 1.

Suzuk,i M., K. Tanemoto and T. Maeda (2003). Aerodynamic characteristics of train/vehicles under cross winds *Journal of Wind Engineering & Industrial* Aerodynamics 91, 209–218.

Xiang, J. and Q. Y. A. Zeng (2005). A study on mechanic mechanism of train derailment and preventive measures for derailment *Vehicle System Dynamic* 43, 121-147.

Xu, H., H. B. Luan, G. H. Tang and W. Q. Tao (2009a). Entropic lattice Boltzmann method for high Reynolds number fluid flows *Progress in Computational Fluid Dynamics* 9, 183-193.

Xu, H., Y. H. Qian and W. Q. Tao (2009b). Revisiting two-dimensional turbulence by lattice Boltzmann method *Progress in Computational Fluid Dynamics* 9, 133-140.

Zhou, L. and Z. Shen (2011). Progress in high-speed train technology around the world *Journal of Modern Transportation* 19, 1-6.

Zou, Q., S. Hou, S. Chen and G. D. Doolen (1995). An improved incompressible lattice Boltzmann model for time-independent flows *Journal of Statistical Physics* 81, 35-48.